

# Sensitivity Analysis of Ectopic Electrical Activity in the Pulmonary Vein Myocardium

Hitomi I Sano<sup>1,2</sup>, Yuichiro Tanaka<sup>1,3</sup>, Yasuhiro Naito<sup>1,2,4</sup>, Masaru Tomita<sup>1,2,4</sup>

<sup>1</sup>Institute for Advanced Biosciences, Keio University, Kanagawa, Japan

<sup>2</sup>Department of Environment and Information Studies, Keio University, Kanagawa, Japan

<sup>3</sup>Department of Policy Management, Keio University, Kanagawa, Japan

<sup>4</sup>Systems Biology Program, Graduate School of Media and Governance, Keio University, Kanagawa, Japan

## Abstract

*The pulmonary vein contains a myocardial layer that is capable of generating spontaneous or triggered action potentials. Although the electrophysiological and pharmacological characteristics of the pulmonary vein myocardium have been compiled in various studies, a comprehensive understanding of the spontaneous action potentials generated in the myocardial layer has yet to be presented. Here we integrated the electrophysiological properties of the pulmonary vein myocardial layer using a guinea pig ventricular cell model. Based on the preceding research, which reported that approximately half of the isolated pulmonary vein myocardial layer exhibited spontaneous action potentials and the remaining half was quiescent, we constructed various combinations of the pulmonary vein myocardial models to represent variations of the action potential tracings. As a result, we predicted that the spontaneous action potentials, including burst-like action potentials, are observed with varying currents of the relative densities of  $\text{Na}^+$  ( $I_{\text{Na}}$ ), L-type  $\text{Ca}^{2+}$  ( $I_{\text{CaL}}$ ), inwardly rectifying  $\text{K}^+$  ( $I_{\text{K1}}$ ), rapid component of delayed rectifying  $\text{K}^+$  ( $I_{\text{Kr}}$ ), and ACh-activated  $\text{K}^+$  ( $I_{\text{KACh}}$ ).*

## 1. Introduction

The myocardial layer of the pulmonary vein (PV) extends from the left atrium but has less negative resting membrane potential due to a lower density of the inwardly rectifying  $\text{K}^+$  current ( $I_{\text{K1}}$ ). Experimental studies reported that approximately half of the isolated PV myocardial layer exhibited a spontaneous action potential and the remaining half was quiescent [1]. Ectopic electrical activity in the PV is considered to play a central role in the generation and maintenance of atrial fibrillation.

Here we integrated electrophysiological properties of the PV myocardial layer [2] on the basis of the guinea pig ventricular cell model, the Kyoto model [3]. We then used the integrated model to predict the model parameter

combinations that resulted in the generation of ectopic electrical activity.

## 2. Methods

Table 1 lists the parameters that we modified in the Kyoto model [3] to represent a myocardial cell in the PV layer; the parameters were estimated based on the electrophysiological recordings of the corresponding ionic channel currents in rabbit PV myocardial cells [2].

Table 1. The list of parameters modified in the Kyoto model [3] used to represent a myocardial cell in the pulmonary vein (PV) layer. We defined the modified model as the PV model.

Parameter (unit)	Ventricular cell	PV
$P_{\text{NaNa}}$ (pA/pF/mM)	21.7	5.1
$P_{\text{NaK}}$ (pA/pF/mM)	2.17	0.51
$P_{\text{CaLCa}}$ (pA/pF/mM)	45.0	10.59
$P_{\text{CaLK}}$ (pA/pF/mM)	0.0164	0.0039
$P_{\text{CaLNa}}$ (pA/pF/mM)	0.0008	0.0002
$G_{\text{K1}}$ (pA/mV)	2.6	0.02123
		7
$G_{\text{Kr}}$ (pA/mV)	0.035	0.02763
$P_{\text{KsK}}$ (pA/pF/mM)	0.025	0.091
$I_{\text{NaCa}}$ amplitude (pA/pF)	110.0	26.65
$G_{\text{KACh}}$ (pA/mV)	0.0	0.135
$C_m$ (pF)	211.2	39.4

Based on the observation that the PV myocardial layer comprises myocardial cells with various electrical activities, we applied our method that we used in a previous study [4] to obtain an overview of the effect of variation in ionic current densities on the generation of spontaneous action potentials. We assumed representing the variation of action potentials within the PV myocardial tissue via generating various combinations of parameters for five different ionic currents:  $\text{Na}^+$  current

( $I_{Na}$ ), L-type  $Ca^{2+}$  current ( $I_{CaL}$ ),  $I_{K1}$ , rapid component of delayed rectifying  $K^+$  current ( $I_{Kr}$ ), and ACh-activated  $K^+$  current ( $I_{KACh}$ ).

All models were first simulated for 600 s, and those combinations that resulted in quiescent membrane potentials were externally stimulated by potassium ions at a frequency of 2.5 Hz for 600 s to pace the model. All simulations were based on the Dormand–Prince method as implemented in E-Cell Simulation Environment version 3 [5].

### 3. Results and discussion

Figure 1 shows the simulated action potentials, dynamics changes in intracellular  $Ca^{2+}$  concentrations, and changes in sarcomere lengths using the original Kyoto model (A) and the PV model (B). The action potential amplitude was shorter in the simulated result with the PV model than in the original Kyoto model. Our simulation showed that the sarcomere shortening amplitude was shorter in the PV model than in the original Kyoto model due to the shorter amplitude of the intracellular  $Ca^{2+}$  transients.

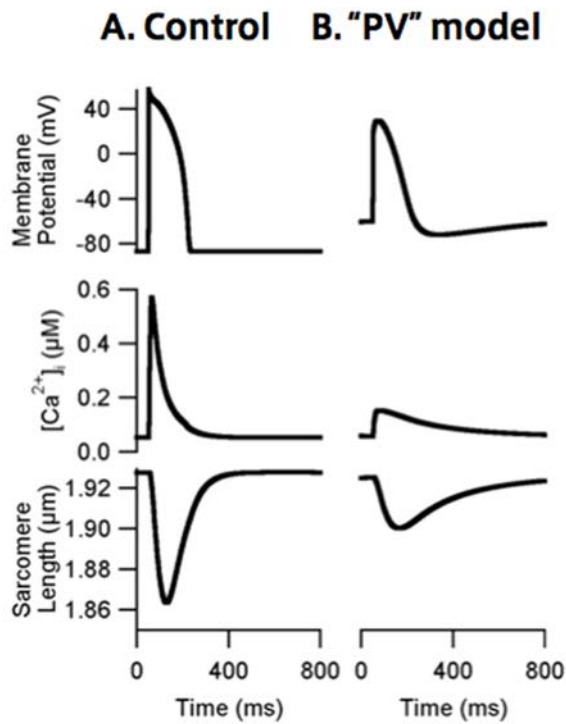


Figure 1. Simulated action potential (mV), intracellular  $Ca^{2+}$  concentration ( $\mu M$ ), and sarcomere length ( $\mu m$ ) in the original Kyoto model (A) and the PV model (B).

Using the PV model, we made 32 combinations of parameters in which relative current densities of  $I_{Na}$ ,  $I_{CaL}$ ,  $I_{K1}$ ,  $I_{Kr}$ , and  $I_{KACh}$  were switched between 0.5 and 2.0. In Figures 2 and 3, the black letters in the white boxes indicate that the relative current density of the corresponding ionic channel current is set to 0.5, whereas the white letters in the black boxes indicate that the relative current density is set to 2.0.

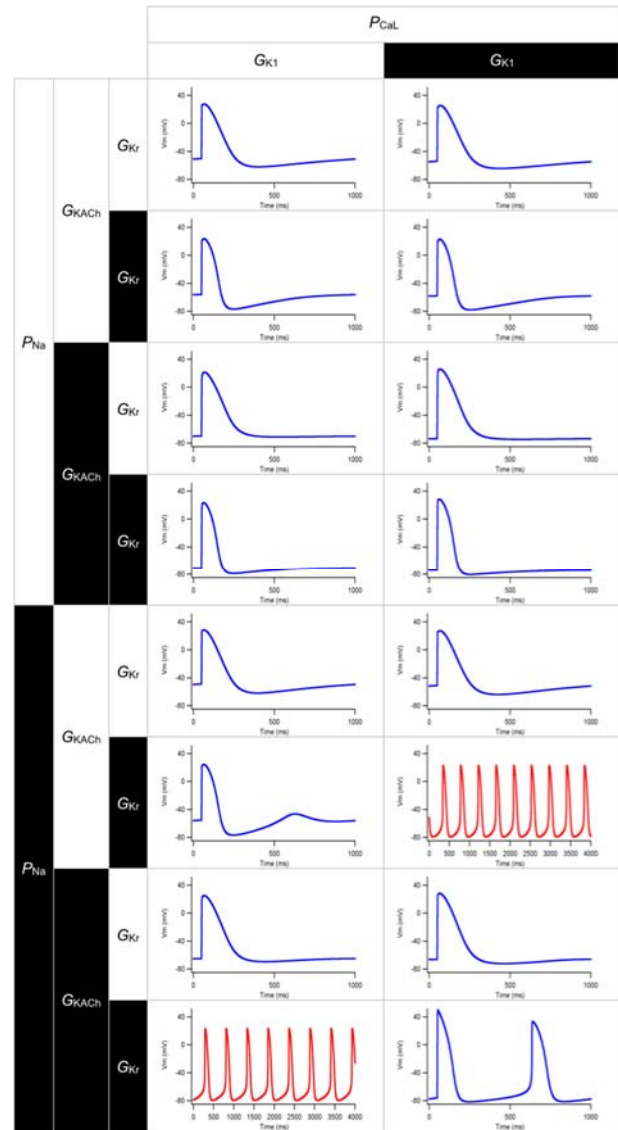


Figure 2. Simulated action potentials of various combinations of relative current densities for  $Na^+$  current ( $P_{Na}$ ), inwardly rectifying  $K^+$  current ( $G_{K1}$ ), rapid component of delayed rectifying  $K^+$  current ( $G_{Kr}$ ), and ACh-activated  $K^+$  current ( $G_{KACh}$ ). The relative current density for L-type  $Ca^{2+}$  current ( $P_{CaL}$ ) was set to 0.5.

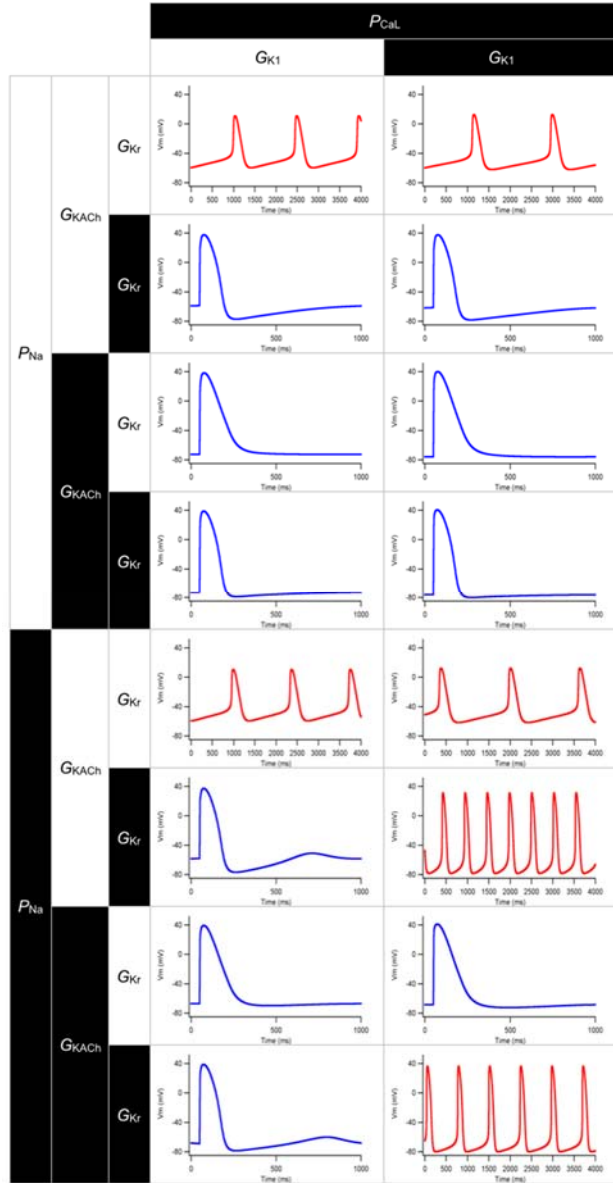


Figure 3. Simulated action potentials of various combinations of relative current densities. The relative current density for L-type  $\text{Ca}^{2+}$  current ( $P_{\text{CaL}}$ ) was set to 2.0.

Of the 32 simulated combinations, eight resulted in spontaneous action potentials (red traces in Figures 2 and 3). For the remaining 24 combinations, an external stimulus was applied to evoke the action potential.

The effects of switching the relative current density for  $I_{K1}$  from 0.5 to 2.0 differed according to the combinations of the relative current densities of the other parameters. In Figure 2, switching of the relative current density for  $I_{K1}$  between 0.5 (black letters in white boxes) and 2.0 (white letters in black boxes) resulted in disappearance of the spontaneous action potential when the relative current

densities of the three other ionic currents ( $I_{\text{Na}}$ ,  $I_{\text{KACh}}$ , and  $I_{\text{Kr}}$ ) were set to 2.0. On the other hand, as we set the relative current density for  $I_{\text{CaL}}$  to 2.0 (Figure 3), the spontaneous action potential appeared as we switched the relative current density for  $I_{K1}$  from 0.5 to 2.0.

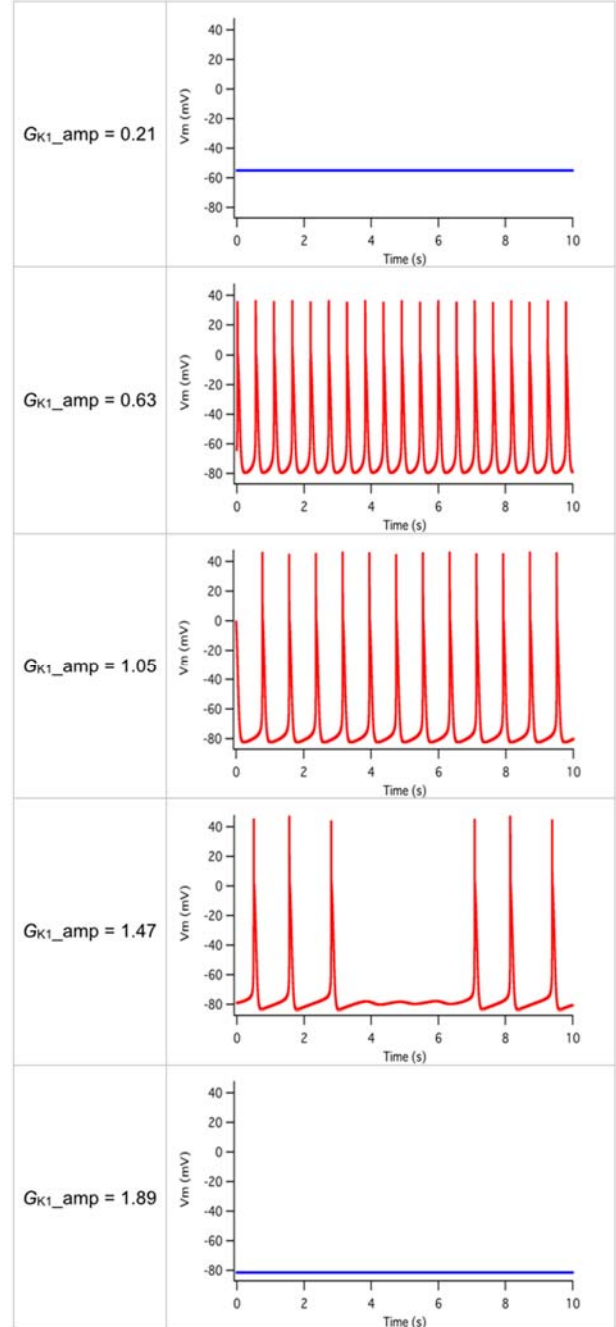


Figure 4. Simulated action potentials at various amplitudes of conductance for  $I_{K1}$  for the parameter combination in which relative current densities for  $I_{\text{Na}}$ ,  $I_{\text{CaL}}$ ,  $I_{\text{Kr}}$ , and  $I_{\text{KACh}}$  were set to 2.0.

To further assess the effect of increasing current density for  $I_{K1}$ , we varied the amplitude of conductance for  $I_{K1}$  with the combination in which relative current densities for  $I_{Na}$ ,  $I_{CaL}$ ,  $I_{Kr}$ , and  $I_{KACh}$  were set to 2.0 (Figure 4). Our simulation showed that the membrane potential was quiescent at approximately -55 mV when the amplitude of  $I_{K1}$  conductance was set to 0.21. Although regular spontaneous action potentials were observed when the amplitude was set to 0.63 and 1.05, the spontaneous action potential became irregular when as we increased the amplitude to 1.47. The membrane potential became quiescent again when we further increased the amplitude to 1.89.

#### 4. Conclusions

Here we integrated the electrophysiological properties of ionic systems in the PV myocardial layer to the Kyoto model. Using the modified model, we made 32 combinations of the model parameters in which the relative current densities for five ionic components varied. As a result, we showed that it is necessary to consider the quantitative changes in current densities for  $I_{Na}$ ,  $I_{CaL}$ ,  $I_{K1}$ ,  $I_{Kr}$ , and  $I_{KACh}$  as combinations because the effect of changing the relative current density for  $I_{K1}$  on the appearance of the spontaneous action potential differed among the combinations of relative current densities for the other four ionic currents.

#### Acknowledgements

This work was supported by funds from the Yamagata Prefectural Government and Tsuruoka City and Keio Gijuku Academic Development Funds. We thank the members of the E-Cell Project at the Institute for Advanced Bioscience, Keio University, for their critical suggestions.

#### References

- [1] Tsuneoka Y, Kobayashi Y, Honda Y, Namekata I, and Tanaka H. Electrical activity of the mouse pulmonary vein myocardium. *J Pharmacol Sci* 2012; 119:287–92.
- [2] Seol CA, Kim, J, Kim, WT, Ha, JM, Choe, H, Jang, YJ, Shim, EB, Youm, JB, Earm, YE, and Leem, CH. Simulation of spontaneous action potentials of cardiomyocytes in pulmonary veins of rabbits. *Prog Biophys Mol Biol* 2008;96:132–51.
- [3] Kuzumoto M, Takeuchi A, Nakai H, Oka C, Noma A, and Matsuoka S. Simulation analysis of intracellular  $Na^+$  and  $Cl^-$  homeostasis during beta 1-adrenergic stimulation of cardiac myocyte. *Prog Biophys Mol Biol* 2008;96:171–86.
- [4] Okubo C, Sano HI, Naito Y, and Tomita M. Contribution of quantitative changes in individual ionic current systems to the embryonic development of ventricular myocytes: a simulation study. *J Physiol Sci* 2013;63:355–67.
- [5] Takahashi K, Kaizu K, Hu B, and Tomita M. A multi-algorithm, multi-timescale method for cell simulation. *Bioinformatics* 2004;20:538–46.

Address for correspondence:

Hitomi I. Sano  
5322 Endo, Fujisawa  
Kanagawa 252-0882, Japan  
ducky@sfc.keio.ac.jp